

## 2023 Update of $\varepsilon_K$ with lattice QCD inputs

---

**Seungyeob Jwa,<sup>a</sup> Jeehun Kim,<sup>a</sup> Sunghee Kim,<sup>a</sup> Sunkyu Lee,<sup>a</sup> Weonjong Lee,<sup>a,b,1,\*</sup> Jaehoon Leem,<sup>c</sup> Jeonghwan Pak<sup>a</sup> and Sungwoo Park<sup>d</sup>**

<sup>a</sup>*Lattice Gauge Theory Research Center, CTP, and FPRD, Department of Physics and Astronomy, Seoul National University, Seoul 08826, South Korea*

<sup>b</sup>*School of Physics, Korea Institute for Advanced Study (KIAS), Seoul 02455, South Korea*

<sup>c</sup>*Computational Science and Engineering Team, Innovation Center, Samsung Electronics, Hwaseong, Gyeonggi-do 18448, South Korea.*

<sup>d</sup>*Lawrence Livermore National Lab, 7000 East Ave, Livermore, CA 94550, USA*

*E-mail:* [wlee@snu.ac.kr](mailto:wlee@snu.ac.kr)

We report recent progress on  $\varepsilon_K$  evaluated directly from the standard model (SM) with lattice QCD inputs such as  $\hat{B}_K$ ,  $|V_{cb}|$ ,  $|V_{us}|$ ,  $|V_{ud}|$ ,  $\xi_0$ ,  $\xi_2$ ,  $\xi_{LD}$ ,  $f_K$ , and  $m_c$ . We find that the standard model with exclusive  $|V_{cb}|$  and lattice QCD inputs describes only 66% of the experimental value of  $|\varepsilon_K|$  and does not explain its remaining 34%, which corresponds to a strong tension in  $|\varepsilon_K|$  at the  $4.9\sigma \sim 3.9\sigma$  level between the SM theory and experiment. We also find that this tension disappears when we use the inclusive value of  $|V_{cb}|$  obtained using the heavy quark expansion based on the QCD sum rule approach.

*The 40th International Symposium on Lattice Field Theory (Lattice 2023)  
July 31st - August 4th, 2023  
Fermi National Accelerator Laboratory*

---

<sup>1</sup>For the SWME collaboration

\*Speaker

## 1. Introduction

This paper is an update of our previous reports [1–8]. We report recent progress in the determination of  $|\varepsilon_K|$  with updated inputs from lattice QCD. Updated input parameters include  $\lambda$ ,  $\bar{\rho}$ ,  $\bar{\eta}$ , exclusive  $|V_{cb}|$ ,  $|V_{us}|$ ,  $|V_{ud}|$ ,  $|V_{us}|/|V_{ud}|$ ,  $M_W$ , and  $M_t$ .

We follow the color convention of our previous papers [1–8] in Tables 1–9. We use red for new input data used to evaluate  $\varepsilon_K$ . We use blue for new input data which is not used.

## 2. Input parameters: Wolfenstein parameters

In Table 1, we summarize results for  $|V_{ud}|$ ,  $|V_{us}|$  from lattice QCD and nuclear  $\beta$  decays, and  $\frac{|V_{us}|}{|V_{ud}|}$  from lattice QCD.

type	$ V_{us} $	$ V_{ud} $	Ref.	type	$ V_{us} / V_{ud} $	Ref.
Lattice $N_f = 2 + 1 + 1$	0.2248(6)	0.97440(15)	FLAG-23 [9]	QCD	0.2313(5)	FLAG-23 [9]
Lattice $N_f = 2 + 1$	<b>0.2249(5)</b>	<b>0.97438(12)</b>	FLAG-23 [9]	QCD+QED	<b>0.2320(5)</b>	FLAG-23 [9]
nuclear $\beta$ decay	0.2278(6)	0.97370(14)	PDG-21 [10]			

(a)  $|V_{us}|$  and  $|V_{ud}|$  from lattice QCD and nuclear  $\beta$  decays

(b)  $|V_{us}|/|V_{ud}|$  from lattice QCD

**Table 1:** (a)  $|V_{us}|$  and  $|V_{ud}|$  (b)  $|V_{us}|/|V_{ud}|$ .

$$\lambda = \frac{|V_{us}|}{\sqrt{|V_{ud}|^2 + |V_{us}|^2}} = \frac{r}{\sqrt{1+r^2}}, \quad r = \frac{|V_{us}|}{|V_{ud}|} \quad (1)$$

Using Eq. (1), we determine  $\lambda$  from  $\frac{|V_{us}|}{|V_{ud}|}$  in Table 1 (b), because its error is less than that obtained by using the values for  $|V_{us}|$  and  $|V_{ud}|$  in Table 1 (a). Results for  $\lambda$  are presented in Table 2 (a), where we summarize the most updated Wolfenstein parameters (WP).

Recently the UTfit collaboration updated values for the WP in Ref. [11]. As explained in Ref. [4, 8], we use the results of the angle-only-fit (AOF) in Table 2 (a) in order to avoid unwanted correlations between  $(\varepsilon_K, |V_{cb}|)$ , and  $(\bar{\rho}, \bar{\eta})$ . We determine the parameter  $A$  from  $|V_{cb}|$ .

WP	CKMfitter	UTfit	AOF	Input	Value	Ref.
$\lambda$	0.22500(24) [12]	<b>0.22519(83)</b> [11, 13]	<b>0.22600(46)</b> [9]	$\eta_{cc}$	1.72(27)	[5]
$\bar{\rho}$	0.1566(85) [12]	<b>0.161(10)</b> [11, 13]	<b>0.156(17)</b> [11]	$\eta_{tt}$	0.5765(65)	[14]
$\bar{\eta}$	0.3475(118) [12]	<b>0.347(10)</b> [11, 13]	<b>0.334(12)</b> [11]	$\eta_{ct}$	0.496(47)	[15]

(a) Wolfenstein parameters

(b)  $\eta_{ij}$

**Table 2:** (a) Wolfenstein parameters and (b) QCD corrections:  $\eta_{ij}$  with  $i, j = c, t$ .

channel	value	method	ref	source
$B \rightarrow D^* \ell \bar{\nu}$	38.40(78)	BGL	[17] p27e76	FNAL/MILC-22
ex-comb	39.48(67)	comb	[9] p195e314	FLAG-23
ex-comb	39.10(50)	comb	[18] p120e221	HFLAV-23
ex-comb	39.31(54)(51)	comb	[19] p22e51	HPQCD-23

(a) Exclusive  $|V_{cb}|$  in units of  $10^{-3}$ .

scheme	value	ref	source
kinetic scheme	42.16(51)	[20] p1	Gambino-21
1S scheme	41.98(45)	[18] p108e200	HFLAV-23

(b) Inclusive  $|V_{cb}|$  in units of  $10^{-3}$ .

**Table 3:** Results for (a) exclusive  $|V_{cb}|$  and (b) inclusive  $|V_{cb}|$ . The abbreviation p27e76 means Eq. (76) on page 27.

### 3. Input parameters: $|V_{cb}|$

In Table 3, we summarize recent updated results for exclusive  $|V_{cb}|$  and inclusive  $|V_{cb}|$ . In Table 3 (a), we present updated results for exclusive  $|V_{cb}|$  obtained by various groups: FNAL/MILC, FLAG, HFLAV, and HPQCD. They are consistent with one another within  $1.0\sigma$  uncertainty.

In Table 3 (b), we present recent updated results for inclusive  $|V_{cb}|$ . There are a number of attempts to determine inclusive  $|V_{cb}|$  from lattice QCD, but all of them at present belong to the category of exploratory study rather than that of precision calculation [16].

### 4. Input parameter $\xi_0$

The absorptive part of long distance effects on  $\varepsilon_K$  is parametrized by  $\xi_0$ .

$$\xi_0 = \frac{\text{Im } A_0}{\text{Re } A_0}, \quad \xi_2 = \frac{\text{Im } A_2}{\text{Re } A_2}, \quad \text{Re} \left( \frac{\varepsilon'}{\varepsilon} \right) = \frac{\omega}{\sqrt{2}|\varepsilon_K|} (\xi_2 - \xi_0). \quad (2)$$

There are two independent methods to determine  $\xi_0$  in lattice QCD: the indirect and direct methods. The indirect method is to determine  $\xi_0$  using Eq. (2) with lattice QCD results for  $\xi_2$  combined with experimental results for  $\varepsilon'/\varepsilon$ ,  $\varepsilon_K$ , and  $\omega$ . The direct method is to determine  $\xi_0$  using the lattice QCD results for  $\text{Im } A_0$ , combined with experimental results for  $\text{Re } A_0$ .

In Table 4 (a), we summarize experimental results for  $\text{Re } A_0$  and  $\text{Re } A_2$ . In Table 4 (b), we summarize lattice results for  $\text{Im } A_0$  and  $\text{Im } A_2$  calculated by RBC-UKQCD. In Table 4 (c), we present results for  $\xi_0$  obtained by using the results in Table 4 (a) and (b).

Here we use the results of the indirect method for  $\xi_0$  to evaluate  $\varepsilon_K$ , since the systematic and statistical errors are much smaller than those of the direct method.

parameter	method	value	Ref.	source
Re $A_0$	exp	$3.3201(18) \times 10^{-7}$ GeV	[21, 22]	NA
Re $A_2$	exp	$1.4787(31) \times 10^{-8}$ GeV	[21]	NA
$\omega$	exp	0.04454(12)	[21]	NA
$ \varepsilon_K $	exp	$2.228(11) \times 10^{-3}$	[10]	PDG-2021
Re ( $\varepsilon'/\varepsilon$ )	exp	$1.66(23) \times 10^{-3}$	[10]	PDG-2021

(a) Experimental results for  $\omega$ , Re  $A_0$  and Re  $A_2$ .

parameter	method	value ( GeV)	Ref.	source
Im $A_0$	lattice	$-6.98(62)(144) \times 10^{-11}$	[23] p4t1	RBC-UK-2020
Im $A_2$	lattice	$-8.34(103) \times 10^{-13}$	[23] p31e90	RBC-UK-2020

(b) Results for Im  $A_0$ , and Im  $A_2$  in lattice QCD.

parameter	method	value	ref	source
$\xi_0$	indirect	$-1.738(177) \times 10^{-4}$	[23]	SWME
$\xi_0$	direct	$-2.102(472) \times 10^{-4}$	[23]	SWME

(c) Results for  $\xi_0$  obtained using the direct and indirect methods in lattice QCD.

**Table 4:** Results for  $\xi_0$ . Here, we use the same notation as in Table 3. The abbreviation p4t1 means Table 1 on page 4.

### 5. Input parameters: $\hat{B}_K$ , $\xi_{LD}$ , and others

The Flavour Lattice Averaging Group (FLAG) [9] reports results for  $\hat{B}_K$  in lattice QCD with  $N_f = 2$ ,  $N_f = 2 + 1$ , and  $N_f = 2 + 1 + 1$ . Here we use the result for  $\hat{B}_K$  with  $N_f = 2 + 1$ , which is obtained by taking an average over the four data points from BMW 11, Laiho 11, RBC-UKQCD 14, and SWME 15 in Table 5 (a).

The dispersive long distance (LD) effect  $\xi_{LD}$  is

$$\xi_{LD} = \frac{m'_{LD}}{\sqrt{2}\Delta M_K}, \quad m'_{LD} = -\text{Im} \left[ \mathcal{P} \sum_C \frac{\langle \bar{K}^0 | H_w | C \rangle \langle C | H_w | K^0 \rangle}{m_{K^0} - E_C} \right] \quad (3)$$

Collaboration	Ref.	$\hat{B}_K$	Input	Value	Ref.
SWME 15	[24]	0.735(5)(36)	$G_F$	$1.1663788(6) \times 10^{-5} \text{ GeV}^{-2}$	PDG-23 [28]
RBC/UKQCD 14	[25]	0.7499(24)(150)	$\theta$	$43.52(5)^\circ$	PDG-23 [28]
Laiho 11	[26]	0.7628(38)(205)	$m_{K^0}$	497.611(13) MeV	PDG-23 [28]
BMW 11	[27]	0.7727(81)(84)	$\Delta M_K$	$3.484(6) \times 10^{-12}$ MeV	PDG-23 [28]
FLAG-23	[9]	0.7625(97)	$F_K$	155.7(3) MeV	FLAG-23 [9]

(a)  $\hat{B}_K$

(b) Other parameters

**Table 5:** (a) Results for  $\hat{B}_K$  and (b) other input parameters.

Collaboration	$N_f$	$m_c(m_c)$	Ref.	Collaboration	$M_t$	$m_t(m_t)$	Ref.
FLAG 2023	2 + 1	1.276(5)	[9]	PDG 2021	172.76(30)	162.96(28)(17)	[10]
FLAG 2023	2 + 1 + 1	1.280(13)	[9]	PDG 2022	172.69(30)	162.90(28)(17)	[28]
				PDG 2023	172.69(30)	162.90(28)(17)	[28]

(a)  $m_c(m_c)$  [GeV] (b)  $m_t(m_t)$  [GeV]

**Table 6:** Results for (a) charm quark mass and (b) top quark mass.

As explained in Ref. [4], there are two independent methods to estimate  $\xi_{LD}$ : one is the BGI estimate [29], and the other is the RBC-UKQCD estimate [30, 31]. The BGI method estimates  $\xi_{LD}$  using chiral perturbation theory, using Eq. (4).

$$\xi_{LD} = -0.4(3) \times \frac{\xi_0}{\sqrt{2}} \tag{4}$$

The RBC-UKQCD method estimates  $\xi_{LD}$  using Eq. (5).

$$\xi_{LD} = (0 \pm 1.6)\% \tag{5}$$

We use both methods to estimate the size of  $\xi_{LD}$ .

In Table 2 (b), we present higher order QCD corrections:  $\eta_{ij}$  with  $i, j = t, c$ . A new approach using  $u - t$  unitarity instead of  $c - t$  unitarity appeared in Ref. [32], which is supposed to have better convergence with respect to the charm quark mass. We are working to incorporate this into our analysis, which we will report soon.

In Table 5 (b), we present other input parameters needed to evaluate  $\varepsilon_K$ . Note that the Fermi coupling constant  $G_F$  has been updated in 2023.

## 6. Quark masses

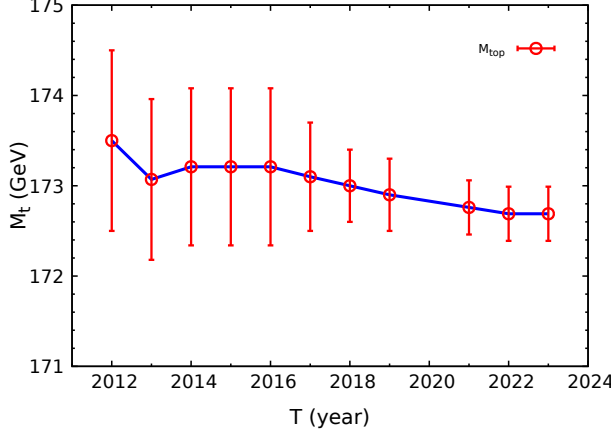
In Table 6 we present the charm quark mass  $m_c(m_c)$  and top quark mass  $m_t(m_t)$ . From FLAG 2023 [9], we take the results for  $m_c(m_c)$  with  $N_f = 2 + 1$ , since there is some inconsistency among the lattice results of various groups with  $N_f = 2 + 1 + 1$ . For the top quark mass, we use the PDG 2023 results for the pole mass  $M_t$  to obtain  $m_t(m_t)$ <sup>1</sup>.

In Table 7 (a) we present the history of values for the top quark pole mass  $M_t$ . We find that the average value shifts downward by 0.47% over time. We also find that the error shrinks fast down to 30% of the original error (2012) thanks to accumulation of high statistics in the LHC experiments. The data for 2020 is dropped out intentionally in memory of the absence of Lattice 2020 due to COVID-19.

## 7. W boson mass

In Fig. 8 (a) we plot  $M_W$  (the  $W$  boson mass) as a function of time. The corresponding results for  $M_W$  are summarized in Table 8 (b). In Fig. 8 (a), the light-green band represents the standard model (SM) prediction, the red circles represent the PDG results from the experimental summary,

<sup>1</sup>Here we use PDG results updated on 2023-5-31.

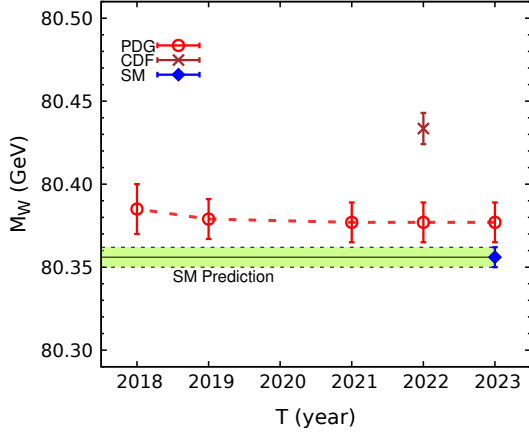


(a) History of  $M_t$  (top quark pole mass).

source	error (%)	memo
$ V_{cb} $	49.6	Exclusive
$\eta_{ct}$	20.7	$c - t$ Box
$\bar{\eta}$	13.3	AOF
$\eta_{cc}$	8.8	$c - c$ Box
$\xi_{LD}$	2.1	RBC-UKQCD
$\bar{\rho}$	2.1	AOF
$\hat{B}_K$	1.7	FLAG
$\vdots$	$\vdots$	$\vdots$

(b) Error budget for  $|\varepsilon_K|^{SM}$

**Table 7:** (a)  $M_t$  history (b) error budget for  $|\varepsilon_K|^{SM}$ .



(a) History of  $M_W$ .

Source	$M_W$ (GeV)	Ref.
SM-2023	80.356(6)	[28]
CDF-2022	80.4335(94)	[33]
PDG-2023	80.377(12)	[28]
PDG-2022	80.377(12)	[28]
PDG-2021	80.377(12)	[10]
PDG-2019	80.379(12)	[34]
PDG-2018	80.385(15)	[35]

(b) Table of  $M_W$ .

**Table 8:**  $W$ -boson mass: (a)  $M_W$  versus time, and (b) table of  $M_W$ .

and the brown cross represents the CDF-2022 result. The upside is that the CDF-2022 result is the most precise experimental result for  $M_W$ . The downside, however, is that it deviates by  $6.9\sigma$  from the standard model prediction (SM-2023). Here we use the SM-2023 result for  $M_W$  to evaluate  $\varepsilon_K$ .

## 8. Results for $\varepsilon_K$

In Fig. 1 we show results for  $|\varepsilon_K|$  evaluated directly from the standard model (SM) with the lattice QCD inputs given in the previous sections. In Fig. 1 (a), the blue curve represents the theoretical evaluation of  $|\varepsilon_K|$  obtained using the FLAG-23 results for  $\hat{B}_K$ , AOF for Wolfenstein parameters, the FNAL/MILC-22 results for exclusive  $|V_{cb}|$ , results for  $\xi_0$  with the indirect method, and the RBC-UKQCD estimate for  $\xi_{LD}$ . The red curve in Fig. 1 represents the experimental results for  $|\varepsilon_K|$ . In Fig. 1 (b), the blue curve represents the theoretical evaluation of  $|\varepsilon_K|$  obtained using the same input parameters as in Fig. 1 (a) except for  $|V_{cb}|$ . Here we use the 1S-scheme results for inclusive  $|V_{cb}|$  instead of those for exclusive  $|V_{cb}|$ .

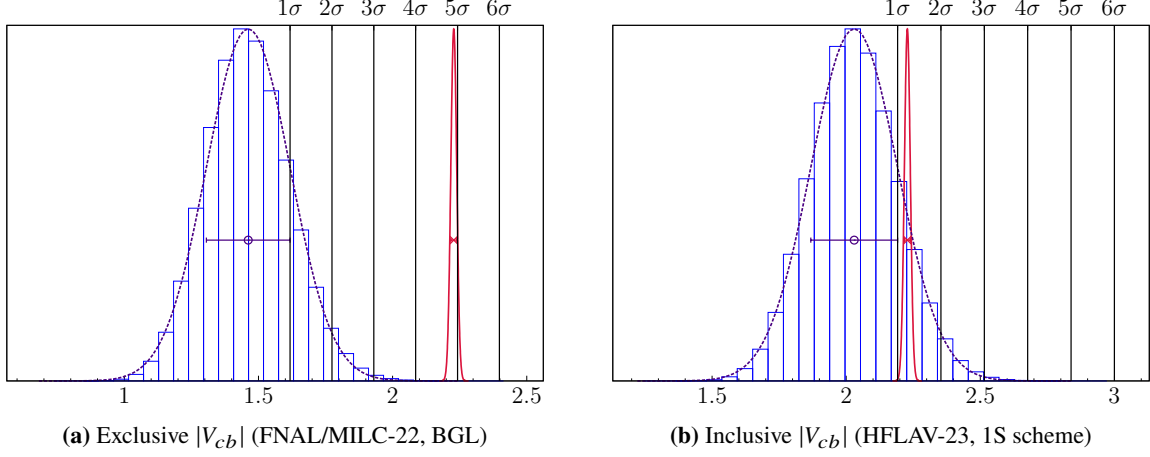


**Figure 1:**  $|\varepsilon_K|$  with (a) exclusive  $|V_{cb}|$  (left) and (b) inclusive  $|V_{cb}|$  (right) in units of  $1.0 \times 10^{-3}$ .

Our results for  $|\varepsilon_K|^{\text{SM}}$  and  $\Delta\varepsilon_K = |\varepsilon_K^{\text{Exp}}| - |\varepsilon_K^{\text{SM}}|$  are summarized in Table 9. Here, the superscript  $^{\text{SM}}$  represents the theoretical expectation value of  $|\varepsilon_K|$  obtained directly from the SM. The superscript  $^{\text{Exp}}$  represents the experimental value of  $|\varepsilon_K| = 2.228(11) \times 10^{-3}$ . Results in Table 9 (a) are obtained using the RBC-UKQCD estimate for  $\xi_{\text{LD}}$ , and those in Table 9 (b) are obtained using the BGI estimate for  $\xi_{\text{LD}}$ . In Table 9 (a), we find that the theoretical expectation values of  $|\varepsilon_K|^{\text{SM}}$  with lattice QCD inputs (with exclusive  $|V_{cb}|$ ) have  $4.9\sigma \sim 3.9\sigma$  tension with the experimental value of  $|\varepsilon_K|^{\text{Exp}}$ , while there is no tension with inclusive  $|V_{cb}|$  (obtained using the heavy quark expansion and QCD sum rules).

In Fig. 2 (a), we show the time evolution of  $\Delta\varepsilon_K/\sigma$  starting from 2012 till 2023. In 2012,  $\Delta\varepsilon_K$  was  $2.5\sigma$ , but now it is  $4.9\sigma$  with exclusive  $|V_{cb}|$  (FNAL/MILC-22, BGL). Here we use the results

$ V_{cb} $	method	source	$ \varepsilon_K ^{\text{SM}}$	$\Delta\varepsilon_K$
exclusive	BGL	FNAL/MILC-22	$1.462 \pm 0.156$	$4.90\sigma$
exclusive	comb	HFLAV-23	$1.561 \pm 0.138$	$4.84\sigma$
exclusive	comb	FLAG-23	$1.619 \pm 0.157$	$3.88\sigma$
exclusive	comb	HPQCD-23	$1.594 \pm 0.162$	$3.90\sigma$
inclusive	1S	HFLAV-23	$2.030 \pm 0.162$	$1.22\sigma$
inclusive	kinetic	Gambino-21	$2.063 \pm 0.169$	$0.98\sigma$

(a)  $|\varepsilon_K|$  with RBC-UKQCD estimate for  $\xi_{\text{LD}}$

$ V_{cb} $	method	reference	$ \varepsilon_K ^{\text{SM}}$	$\Delta\varepsilon_K$
exclusive	BGL	FNAL/MILC-21	$1.510 \pm 0.159$	$4.52\sigma$
exclusive	comb	HFLAV-23	$1.609 \pm 0.140$	$4.41\sigma$

(b)  $|\varepsilon_K|$  with BGI estimate for  $\xi_{\text{LD}}$

**Table 9:**  $|\varepsilon_K|$  in units of  $1.0 \times 10^{-3}$ , and  $\Delta\varepsilon_K = |\varepsilon_K|^{\text{Exp}} - |\varepsilon_K|^{\text{SM}}$  in units of  $\sigma$ .

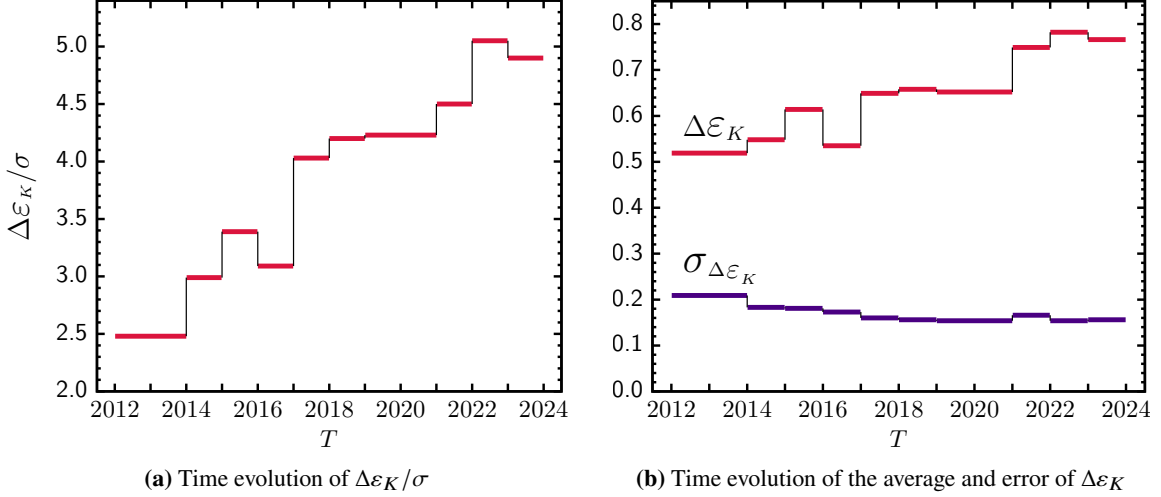


**Figure 2:** Time history of (a)  $\Delta\varepsilon_K/\sigma$ , and (b)  $\Delta\varepsilon_K$  and  $\sigma_{\Delta\varepsilon_K}$ .

for exclusive  $|V_{cb}|$  from FNAL/MILC-22, since it contains the most comprehensive analysis of the  $\bar{B} \rightarrow D^* \ell \bar{\nu}$  decays at both zero recoil and non-zero recoil, while it incorporates both BELLE and BABAR experimental results. In Fig. 2 (b) we show the time evolution of the average  $\Delta\varepsilon_K$  and the error  $\sigma_{\Delta\varepsilon_K}$  during the period of 2012–2023.

At present we find  $|V_{cb}|$  gives the largest error ( $\approx 50\%$ ) in  $|\varepsilon_K|^{\text{SM}}$ . Refer to Table 7 (b) for more details. Hence, it is essential to reduce the errors in  $|V_{cb}|$  as much as possible. Part of the errors come from experiments in BELLE, BELLE2, BABAR, and LHCb, which are beyond our control but will decrease thanks to on-going accumulation of higher statistics in BELLE2 and LHCb. Part of the errors come from the theory used to evaluate the semi-leptonic form factors for  $\bar{B} \rightarrow D^{(*)} \ell \bar{\nu}$  decays, using the tools of lattice QCD. In order to reduce the errors on the theoretical side, there is an on-going project to determine exclusive  $|V_{cb}|$  using the Oktay-Kronfeld (OK) action for the heavy quarks to calculate the form factors for  $\bar{B} \rightarrow D^{(*)} \ell \bar{\nu}$  decays [36–42].

A large portion of interesting results for  $|\varepsilon_K|^{\text{SM}}$  and  $\Delta\varepsilon_K$  could not be presented in Table 9 and in Fig. 2 due to lack of space: For example, results for  $|\varepsilon_K|^{\text{SM}}$  obtained using exclusive  $|V_{cb}|$  (FLAG-23) with the BGI estimate for  $\xi_{\text{LD}}$ , results for  $|\varepsilon_K|^{\text{SM}}$  obtained using  $\xi_0$  determined by the direct method, and so on. We plan to report them collectively in Ref. [43]. We find that there was another analysis on  $\varepsilon_K$  in Ref. [44].

## Acknowledgments

We thank J. Bailey, Y.C. Jang, S. Sharpe, and R. Gupta for helpful discussion. We thank G. Martinelli for providing us with the most updated results of the UTfit Collaboration in time. The research of W. Lee is supported by the Mid-Career Research Program (Grant No. NRF-2019R1A2C2085685) of the NRF grant funded by the Korean government (MSIT). W. Lee would like to acknowledge the support from the KISTI supercomputing center through the strategic support program for the supercomputing application research (No. KSC-2018-CHA-0043, KSC-2020-CHA-0001, KSC-2023-CHA-0010). Computations were carried out in part on the DAVID cluster at Seoul National University.



## References

- [1] **SWME Collaboration**, W. Lee, S. Kim, S. Lee, J. Leem, and S. Park, *2022 update on  $\varepsilon_K$  with lattice QCD inputs*, *PoS LATTICE2022* (2023) 297, [[2301.12375](#)].
- [2] **SWME Collaboration**, W. Lee, J. Kim, Y.-C. Jang, S. Lee, J. Leem, C. Park, and S. Park, *2021 update on  $\varepsilon_K$  with lattice QCD inputs*, *PoS LATTICE2021* (2021) 078, [[2202.11473](#)].
- [3] **LANL-SWME Collaboration**, J. Kim, S. Lee, W. Lee, Y.-C. Jang, J. Leem, and S. Park *PoS LATTICE2019* (2019) 029, [[1912.03024](#)].
- [4] J. A. Bailey *et al.* *Phys. Rev.* **D98** (2018) 094505, [[1808.09657](#)].
- [5] J. A. Bailey, Y.-C. Jang, W. Lee, and S. Park *Phys. Rev.* **D92** (2015) 034510, [[1503.05388](#)].
- [6] J. A. Bailey *et al.* *PoS LATTICE2018* (2018) 284, [[1810.09761](#)].
- [7] Y.-C. Jang, W. Lee, S. Lee, and J. Leem *EPJ Web Conf.* **175** (2018) 14015, [[1710.06614](#)].
- [8] J. A. Bailey, Y.-C. Jang, W. Lee, and S. Park *PoS LATTICE2015* (2015) 348, [[1511.00969](#)].
- [9] **Flavour Lattice Averaging Group (FLAG) Collaboration**, Y. Aoki *et al.* *Eur. Phys. J. C* **82** (2022), no. 10 869, [[2111.09849](#)].
- [10] **Particle Data Group Collaboration**, P. Zyla *et al.* *PTEP* **2020** (2020), no. 8 083C01.
- [11] **UTfit Collaboration**, M. Bona *et al.*, *New UTfit Analysis of the Unitarity Triangle in the Cabibbo-Kobayashi-Maskawa scheme*, *Rend. Lincei Sci. Fis. Nat.* **34** (2023) 37–57, [[2212.03894](#)].
- [12] J. Charles *et al.* *Eur.Phys.J.* **C41** (2005) 1–131, [[hep-ph/0406184](#)]. updated results and plots available at: <http://ckmfitter.in2p3.fr>.
- [13] M. Bona *et al.* *JHEP* **10** (2006) 081, [[hep-ph/0606167](#)]. Standard Model fit results: Summer 2016 (ICHEP 2016): <http://www.utfit.org>.
- [14] A. J. Buras and D. Guadagnoli *Phys.Rev.* **D78** (2008) 033005, [[0805.3887](#)].
- [15] J. Brod and M. Gorbahn *Phys.Rev.* **D82** (2010) 094026, [[1007.0684](#)].
- [16] A. Barone, A. Jüttner, S. Hashimoto, T. Kaneko, and R. Kellermann, *Inclusive semi-leptonic  $B_{(s)}$  mesons decay at the physical  $b$  quark mass*, *PoS LATTICE2022* (2023) 403, [[2211.15623](#)].
- [17] **Fermilab Lattice, MILC Collaboration**, A. Bazavov *et al.* *Eur. Phys. J. C* **82** (2022), no. 12 1141, [[2105.14019](#)].
- [18] **Heavy Flavor Averaging Group, HFLAV Collaboration**, Y. S. Amhis *et al.*, *Averages of  $b$ -hadron,  $c$ -hadron, and  $\tau$ -lepton properties as of 2021*, *Phys. Rev. D* **107** (2023), no. 5 052008, [[2206.07501](#)].

- [19] J. Harrison and C. T. H. Davies,  $B \rightarrow D^*$  vector, axial-vector and tensor form factors for the full  $q^2$  range from lattice QCD, [2304.03137](#).
- [20] M. Bordone, B. Capdevila, and P. Gambino *Phys. Lett. B* **822** (2021) 136679, [[2107.00604](#)].
- [21] T. Blum *et al.* *Phys. Rev.* **D91** (2015) 074502, [[1502.00263](#)].
- [22] Z. Bai *et al.* *Phys. Rev. Lett.* **115** (2015) 212001, [[1505.07863](#)].
- [23] **RBC, UKQCD** Collaboration, R. Abbott *et al.* *Phys. Rev. D* **102** (2020), no. 5 054509, [[2004.09440](#)].
- [24] B. J. Choi *et al.* *Phys. Rev.* **D93** (2016) 014511, [[1509.00592](#)].
- [25] T. Blum *et al.* *Phys. Rev.* **D93** (2016) 074505, [[1411.7017](#)].
- [26] J. Laiho and R. S. Van de Water *PoS LATTICE2011* (2011) 293, [[1112.4861](#)].
- [27] S. Durr *et al.* *Phys. Lett.* **B705** (2011) 477–481, [[1106.3230](#)].
- [28] **Particle Data Group** Collaboration, R. L. Workman and Others *PTEP* **2022** (2022) 083C01.
- [29] A. J. Buras, D. Guadagnoli, and G. Isidori *Phys. Lett.* **B688** (2010) 309–313, [[1002.3612](#)].
- [30] N. Christ *et al.* *Phys. Rev.* **D88** (2013) 014508, [[1212.5931](#)].
- [31] N. Christ *et al.* *PoS LATTICE2013* (2014) 397, [[1402.2577](#)].
- [32] J. Brod, M. Gorbahn, and E. Stamou *Phys. Rev. Lett.* **125** (2020), no. 17 171803, [[1911.06822](#)].
- [33] **CDF** Collaboration, T. Aaltonen *et al.* *Science* **376** (2022), no. 6589 170–176.
- [34] M. Tanabashi *et al.* *Phys. Rev.* **D98** (2018) 030001. <http://pdg.lbl.gov/2019/>.
- [35] C. Patrignani *et al.* *Chin. Phys.* **C40** (2016) 100001. <https://pdg.lbl.gov/>.
- [36] T. Bhattacharya, B. J. Choi, R. Gupta, Y.-C. Jang, S. Jwa, S. Lee, W. Lee, J. Leem, S. Park, and B. Yoon *PoS LATTICE2021* (2021) 136, [[2204.05848](#)].
- [37] **LANL-SWME** Collaboration, S. Park, T. Bhattacharya, R. Gupta, Y.-C. Jang, B. J. Choi, S. Jwa, S. Lee, W. Lee, and J. Leem *PoS LATTICE2019* (2020) 050, [[2002.04755](#)].
- [38] **LANL/SWME** Collaboration, T. Bhattacharya, B. J. Choi, R. Gupta, Y.-C. Jang, S. Jwa, S. Lee, W. Lee, J. Leem, and S. Park *PoS LATTICE2019* (2020) 056, [[2003.09206](#)].
- [39] T. Bhattacharya *et al.* *PoS LATTICE2018* (2018) 283, [[1812.07675](#)].
- [40] J. A. Bailey *et al.* *EPJ Web Conf.* **175** (2018) 13012, [[1711.01786](#)].
- [41] J. Bailey, Y.-C. Jang, W. Lee, and J. Leem *EPJ Web Conf.* **175** (2018) 14010, [[1711.01777](#)].

- 
- [42] **LANL-SWME** Collaboration, J. A. Bailey, Y.-C. Jang, S. Lee, W. Lee, and J. Leem *Phys. Rev. D* **105** (2022), no. 3 034509, [[2001.05590](#)].
- [43] **SWME** Collaboration, J. Bailey, J. Kim, S. Lee, W. Lee, Y.-C. Jang, J. Leem, S. Park, *et al.* in preparation.
- [44] A. J. Buras and E. Venturini, *The exclusive vision of rare K and B decays and of the quark mixing in the standard model*, *Eur. Phys. J. C* **82** (2022), no. 7 615, [[2203.11960](#)].